

Supporting Information

Planarized intramolecular charge transfer on triphenylamine-modified pyrazine and their application in organic light-emitting diodes

Bing Zhang, Haozhong Wu, Zhiming Wang*, Anjun Qin, Ben Zhong Tang*

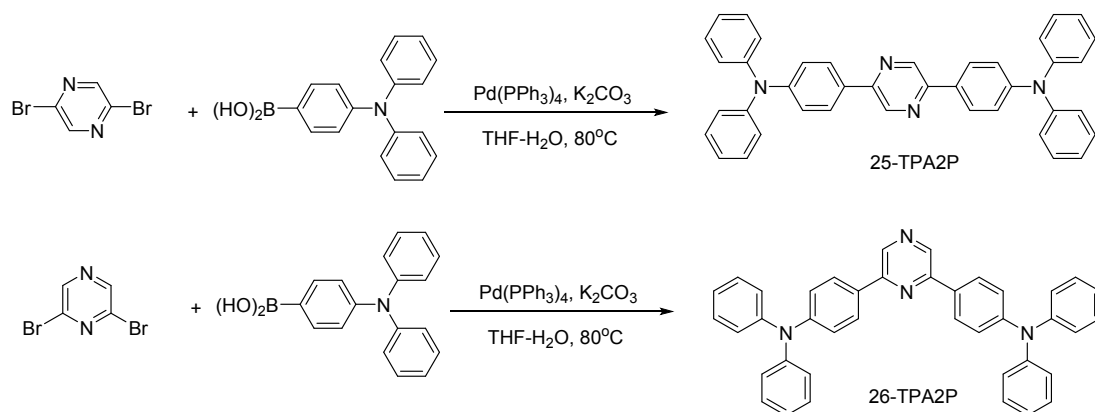
1. General Information

THF was distilled with sodium and benzophenone under dry N₂ before using. All other chemicals and reagents were purchased from commercial sources and used as received without further purification. ¹H and ¹³C NMR spectra were measured on a VNMR5 500 spectrometer. High resolution mass spectra (HRMS) were recorded on a GCT premier CAB048 mass spectrometer operating in MALDI-TOF mode. Absorption spectrum were tested on a Shimadzu UV-2600 spectrophotometer. Photoluminescence (PL) spectrum were measured on a Horiba Fluoromax-4 spectrofluorometer. Fluorescence quantum yields were characterized using a Hamamatsu absolute PL quantum yield spectrometer C11347 Quantaaurus QY. Fluorescence lifetimes were determined with a Hamamatsu C11367-11 Quantaaurus-Tau time-resolved spectrometer. The geometries were optimized using the (time dependent) density functional theory ((TD)DFT) method with M06-2X/6-31G (d, p) level performing on Gaussian 09 package. Thermogravimetric analysis (TGA) analysis was performed on a TA TGA Q5000 under dry nitrogen at a heating rate of 20 °C min⁻¹ and Differential scanning calorimetry (DSC) analysis was carried out on a DSC Q1000 under dry nitrogen at a heating rate of 10 °C min⁻¹. Cyclic voltammetry (CV) were performed on a BAS 100W Bioanalytical Systems, using a platinum wire as the auxiliary electrode, a glass carbon disk as the working electrode and Ag/Ag⁺ as the reference electrode, standardized for the redox couple ferricinium/ferrocene (Fc/Fc⁺).

2. Device Fabrication

Glass substrates pre-coated with a 95-nm-thin layer of indium tin oxide (ITO) with a sheet resistance of 20 Ω per square were thoroughly cleaned for 10 minutes in ultrasonic bath of acetone, isopropyl alcohol, detergent, deionized water, and isopropyl alcohol. Then, the substrates were totally dried in a 75 °C oven. After that, in order to improving the hole injection ability of ITO, the substrates were treated by O₂ plasma for 10 minutes. Multilayer OLEDs were fabricated by the vacuum-deposition method. Organic layers were deposited by high-vacuum (~5 × 10⁻⁴ Pa) thermal evaporation onto a glass substrate pre-coated with an ITO layer. All organic layers were deposited sequentially. The thermal deposition rates for the organic materials, LiF and Al were 1.0~1.5, 0.1 and 3~5 Å s⁻¹, respectively. The active area of each device was 9 mm². The electroluminescence spectra, the current density-voltage characteristics and the current density-voltage-luminance curves characterizations of the OLEDs were carried out with a Photo Research SpectraScan PR-745 Spectroradiometer and a Keithley 2450 Source Meter and they are recorded simultaneously. All measurements were done at room temperature under ambient conditions.

3. Synthesis and Characterization



Scheme S1. The synthesis route of two pyrazine compounds.

4,4'-(pyrazine-2,5-diyl)bis(N,N-diphenylaniline) (25-TPA2P): A mixture of 2,5-dibromopyrazine (3 mmol, 710 mg), 4-(diphenylamino)phenylboronic acid (9 mmol, 2630 mg), Pd(PPh₃)₄ (0.3 mmol, 350 mg) and K₂CO₃ (13.5 mmol, 1860 mg) was added in 100 mL two-neck bottle under nitrogen. After then, a mixed solvent system of THF/water (v/v = 7:3) 30 mL was injected into the bottle and the mixture was refluxed at 80 °C overnight under nitrogen atmosphere. After cooling to room temperature, the mixture was poured into water and extracted with dichloromethane three times and the combined organic layers were washed with brine, and then dried over MgSO₄. The solvent was removed under reduced pressure and the crude product was purified by column chromatography, yield was 78%. ¹H NMR (500 MHz, CD₂Cl₂) δ 8.96 (s, 2H), 7.98 – 7.90 (m, 4H), 7.35 – 7.25 (m, 8H), 7.18 – 7.06 (m, 16H). ¹³C NMR (126 MHz, CD₂Cl₂) δ 149.86, 149.83, 147.83, 140.94, 130.14, 129.99, 127.91, 125.69, 124.23, 123.06. HRMS (C₄₀H₃₀N₄): *m/z* 566.2470 (M⁺, calcd 566.2440).

Crystal data for 25-TPA2P (CCDC 1976105): C₄₀H₃₀N₄, *MW* = 566.68, triclinic, P-1, *a* = 9.1562(9) Å, *b* = 11.5073(9) Å, *c* = 16.3445(15) Å, *α* = 96.786(3)°, *β* = 95.303(3)°, *γ* = 103.339(3)°, *V* = 1651.1(1) Å³, *Z* = 2, *D_c* = 1.140 g cm⁻³, *μ* = 0.067 mm⁻¹ (MoKα, *λ* = 0.71073), *F*(000) = 596, *T* = 173(2) K, 2*θ*_{max} = 25.242° (99.1%), 13291 measured reflections, 6009 independent reflections (*R*_{int} = 0.0761), GOF on *F*² = 1.050, *R*₁ = 0.1400, *wR*₂ = 0.1076 (all data), *Δe* 0.177 and -0.208 eÅ⁻³.

4,4'-(pyrazine-2,6-diyl)bis(N,N-diphenylaniline) (26-TPA2P): A mixture of 2,6-dibromopyrazine (2 mmol, 470 mg), 4-(diphenylamino)phenylboronic acid (8mmol, 2340 mg), Pd(PPh₃)₄ (0.2 mmol, 230 mg) and K₂CO₃ (16 mmol, 2200 mg) was added in 100 mL two-neck bottle under nitrogen. After then, a mixed solvent system of THF/water (v/v = 7:3) 30 mL was injected into the bottle and the mixture was refluxed at 80 °C overnight under nitrogen atmosphere. After cooling to room temperature, the mixture was poured into water and extracted with dichloromethane three times and the combined organic layers were washed with brine, and then dried over MgSO₄. The solvent was removed under reduced pressure and the crude product was purified by column chromatography, yield was 72%. ¹H NMR (500 MHz, CD₂Cl₂) δ 8.84 – 8.80 (m, 2H), 8.03 – 7.98 (m, 4H), 7.34 – 7.27 (m, 8H), 7.18 – 7.12 (m, 12H), 7.11 – 7.05 (m, 4H). ¹³C NMR (126 MHz, CD₂Cl₂) δ 151.47, 150.08, 147.83, 139.01, 130.38, 129.99, 128.29, 125.70, 124.25, 122.98. HRMS (C₄₀H₃₀N₄): *m/z* 566.2470 (M⁺, calcd 566.2452).

Crystal data for 26-TPA2P (CCDC 1976102): $C_{40}H_{30}N_4$, $MW = 566.68$, monoclinic, $P21/C$, $a = 10.83112(13)$ Å, $b = 17.04215(19)$ Å, $c = 16.50807(19)$ Å, $\alpha = 90^\circ$, $\beta = 105.5618(13)^\circ$, $\gamma = 90^\circ$, $V = 2935.45(6)$ Å³, $Z = 4$, $D_c = 1.282$ g cm⁻³, $\mu = 0.587$ mm⁻¹ (CuK α , $\lambda = 1.54184$), $F(000) = 1192$, $T = 150.00(10)$ K, $2\theta_{max} = 67.078^\circ$ (99.3%), 16056 measured reflections, 5207 independent reflections ($R_{int} = 0.0232$), GOF on $F^2 = 1.058$, $R_1 = 0.0383$, $wR_2 = 0.0916$ (all data), Δe 0.144 and -0.207 eÅ⁻³.

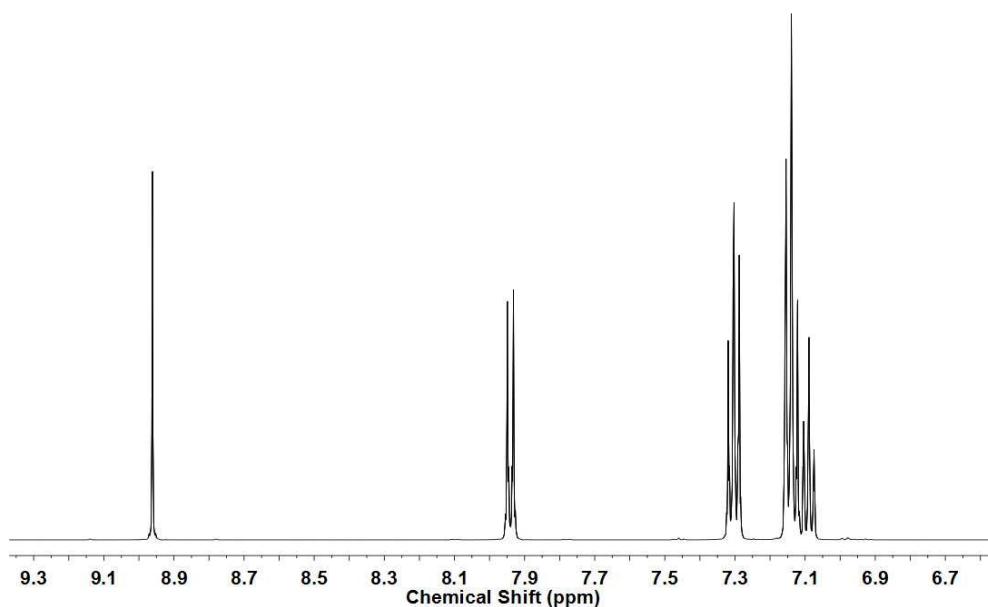


Fig. S1 The ¹H-NMR spectrum of 25-TPA2P in CD₂Cl₂.

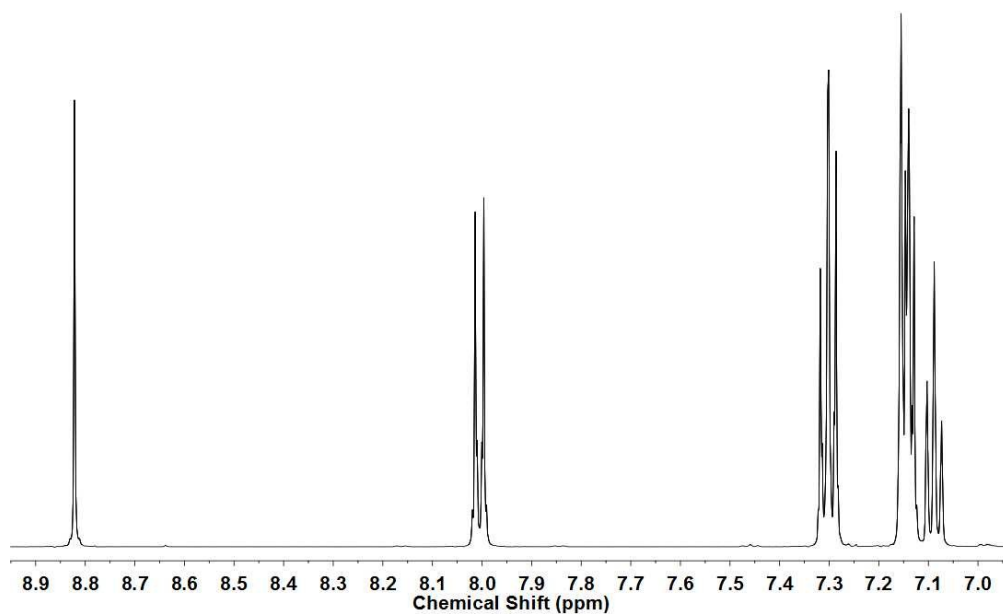


Fig. S2 The ¹H-NMR spectrum of 26-TPA2P in CD₂Cl₂.

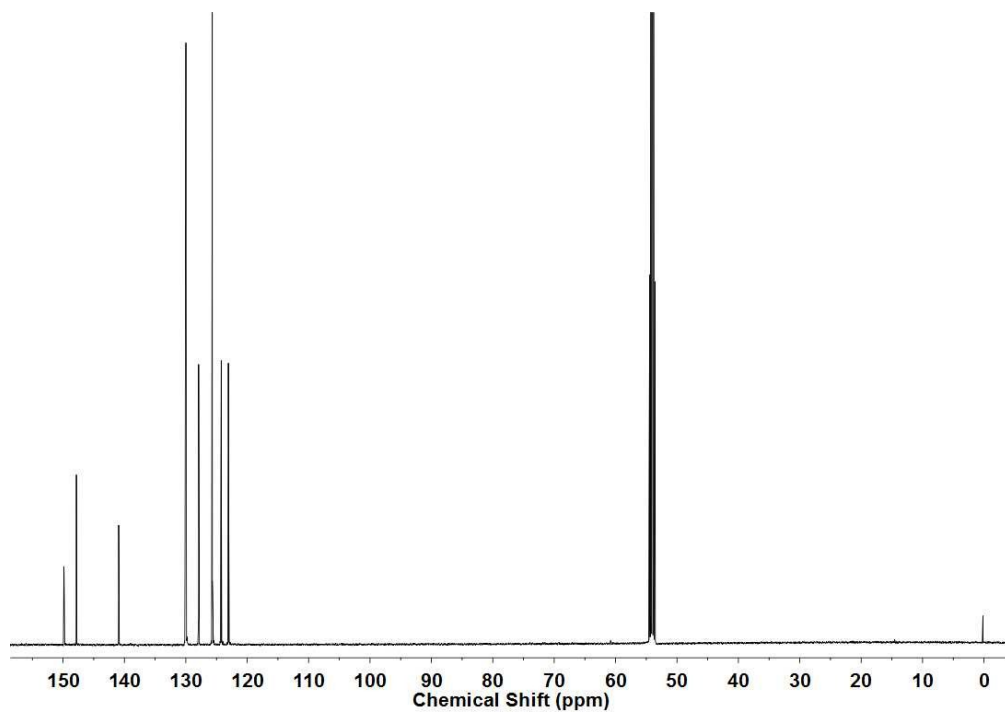


Fig. S3 The ^{13}C -NMR spectrum of 25-TPA2P in CD_2Cl_2 .

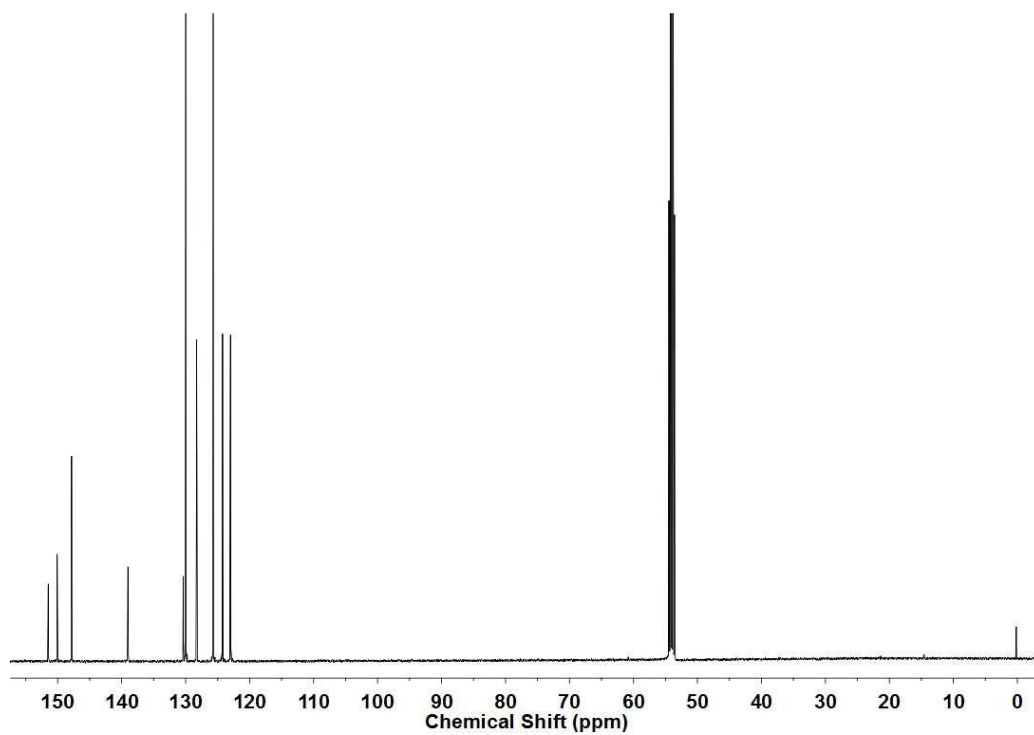


Fig. S4 The ^{13}C -NMR spectrum of 26-TPA2P in CD_2Cl_2 .

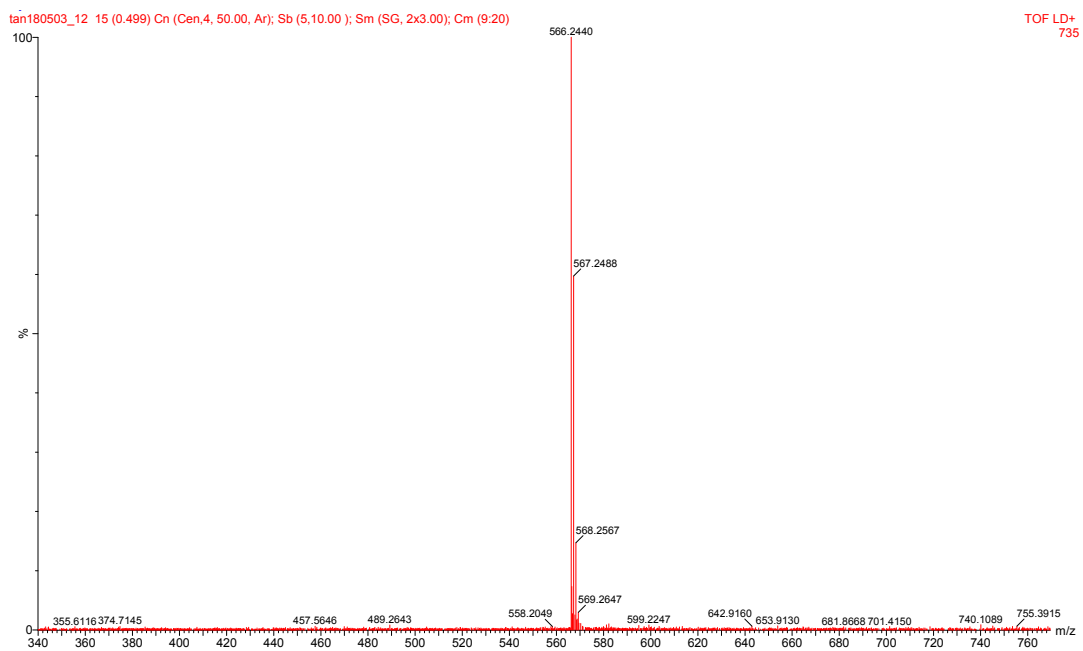


Fig. S5 The HRMS spectrum of 25-TPA2P.

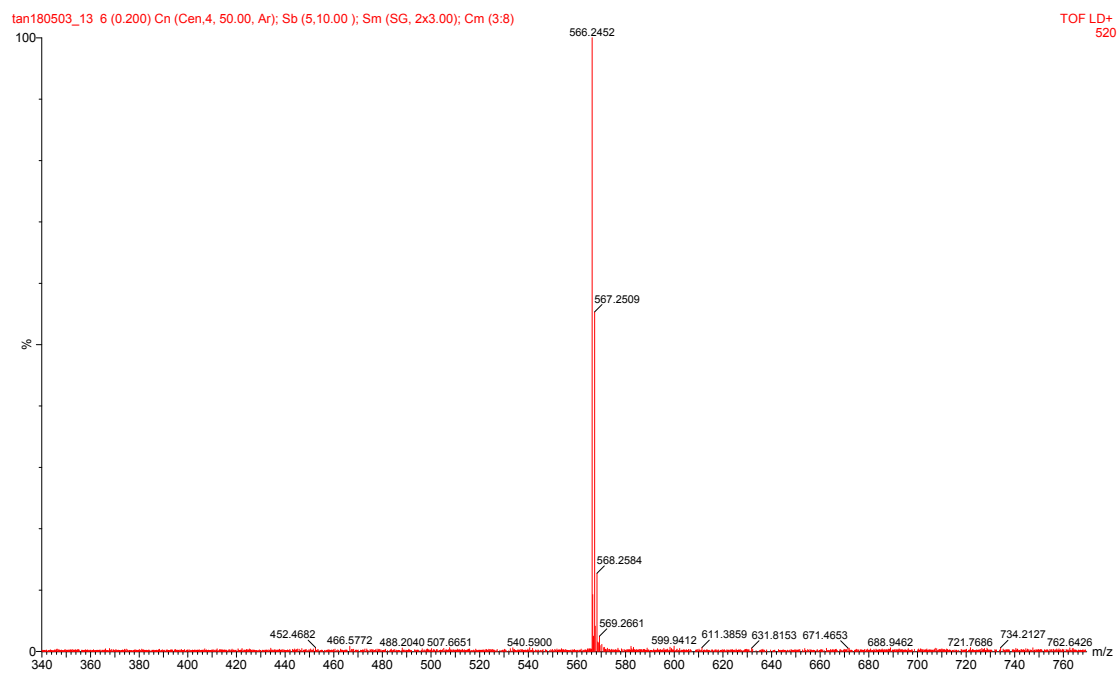


Fig. S6 The HRMS spectrum of 26-TPA2P.

4. Characterization of Thermogravimetric, Electrochemical and photophysics properties

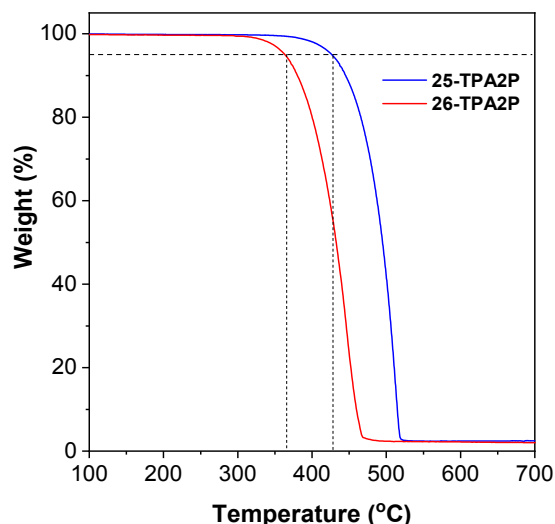


Fig. S7 The TGA curve of 25-TPA2P and 26-TPA2P.

Table S1. The value of T_d , HOMO, LUMO and E_{gap} for two compounds.

Compounds	T_d (°C)	HOMO (eV) ^a	LUMO (eV) ^a	E_{gap} (eV) ^b
25-TPA2P	425	-5.22	-2.59	2.63
26-TPA2P	363	-5.12	-2.48	2.64

^a Determined by CV measurement: $E_{\text{HOMO}} = -(E_{\text{ox}} - E_{(1/2) \text{Fc/Fc}^+} + 4.8)$ eV, $E_{(1/2) \text{Fc/Fc}^+} = 0.42$ eV. ^b Calculated from the formula: $E_{\text{HOMO}} = E_{\text{LUMO}} + E_{\text{gap}}$.

Table S2. The photophysical properties of 25-TPA2P.

Solvents	ϵ	n	$f(\epsilon, n)$				Φ (%)	τ (ns)
				λ_a (nm)	λ_f (nm)	$\nu_a - \nu_f$ (cm^{-1})		
Toluene	2.4	1.496	0.0015	405	452	2616	86.2	1.46
Ethyl acetate	6.02	1.372	0.2	400	463	3402	85.7	1.86
Tetrahydrofuran	7.58	1.407	0.21	404	466	3293	87.9	1.86
Dichloromethane	8.93	1.424	0.217	406	488	4139	93.9	2.34
Dimethyl formamide	37	1.427	0.276	406	498	4550	92.0	2.86

Table S3. The photophysical properties of 26-TPA2P.

Solvents	ϵ	n	$f(\epsilon, n)$				Φ (%)	τ (ns)
				λ_a (nm)	λ_f (nm)	$\nu_a - \nu_f$ (cm^{-1})		
Toluene	2.4	1.496	0.0015	386	430	2651	66.3	2.15
Ethyl acetate	6.02	1.372	0.2	381	448	3925	63.5	3.11
Tetrahydrofuran	7.58	1.407	0.21	383	450	3887	67.0	3.15
Dichloromethane	8.93	1.424	0.217	385	479	5097	69.7	4.36
Dimethyl formamide	37	1.427	0.276	385	495	5772	68.2	5.88

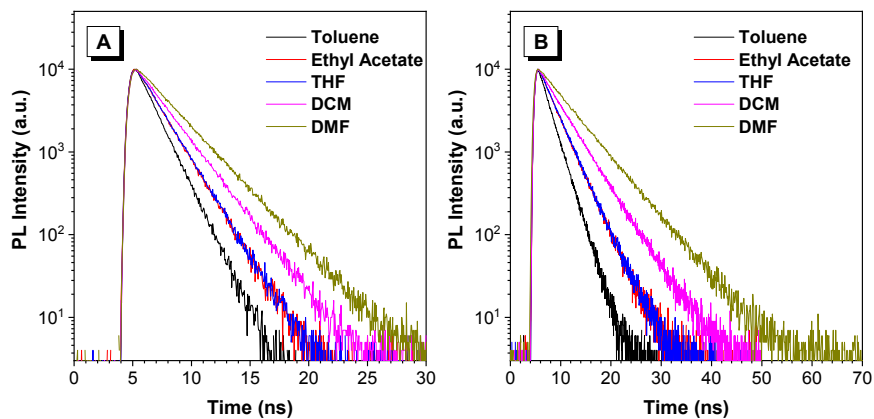


Fig. S8 Transient decay spectra of 25-TPA2P (A) and 26-TPA2P (B) in different solvents with various polarity ($10 \mu\text{M}$).

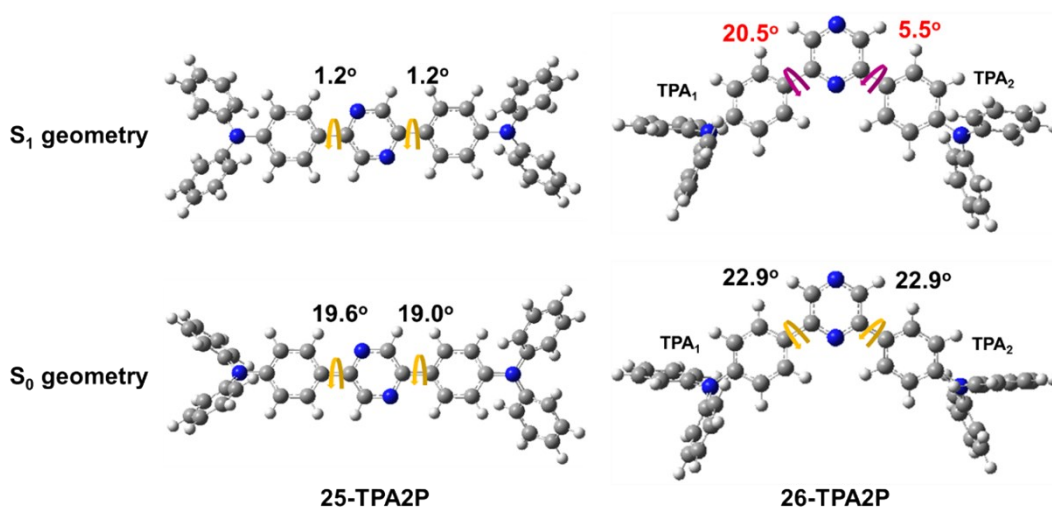
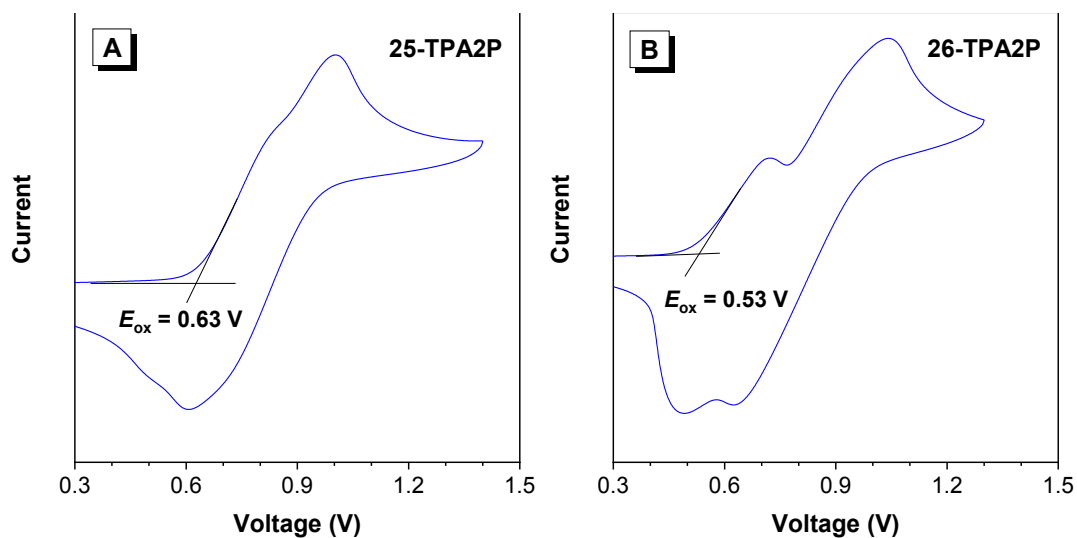


Fig. S9 The S_0 and S_1 geometries of 25-TPA2P and 26-TPA2P.



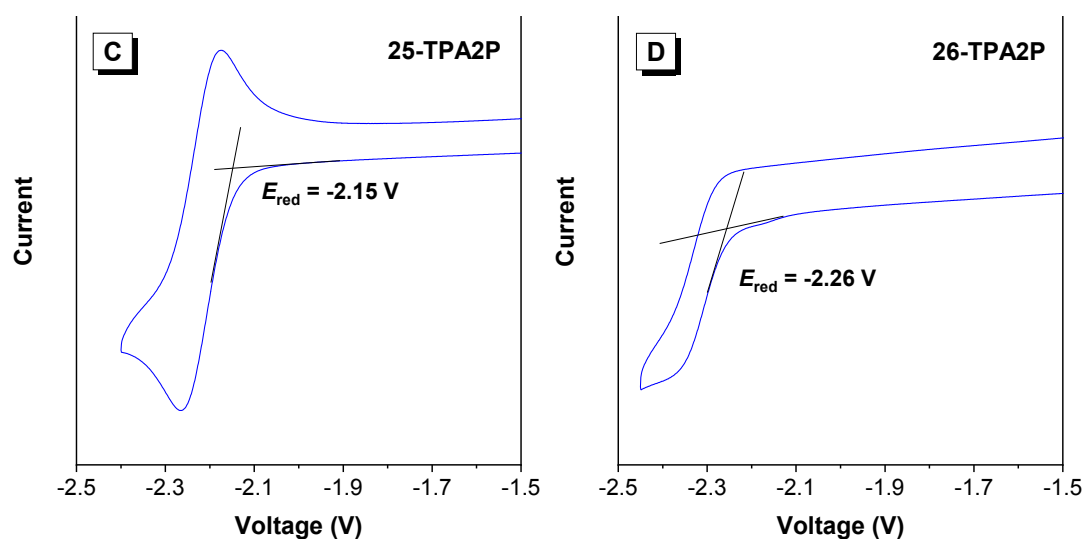


Fig. S10 The CV curve of oxidation part for (A) 25-TPA2P and (B) 26-TPA2P in dichloromethane; The CV curve of reduction part for (C) 25-TPA2P and (D) 26-TPA2P in DMF.

5. Supplementary Fig.s and Tables of EL Devices

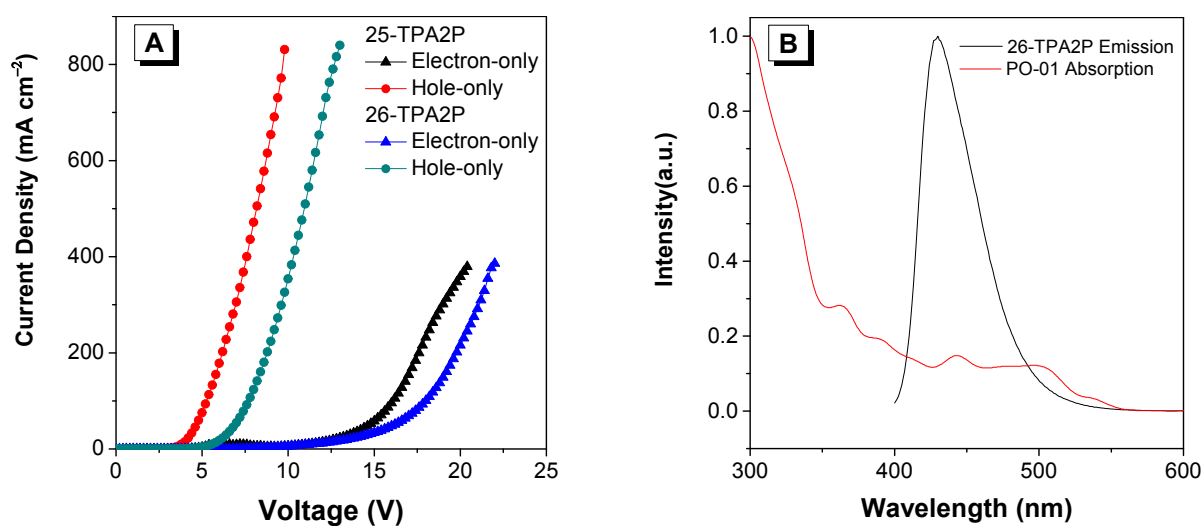


Fig. S11 (A) Current density changed curves with the change of voltage (J - V) of the devices of 25-TPA2P and 26-TPA2P. Device configuration: ITO/TmPyPB (10 nm)/Host (80 nm)/LiF (1 nm)/Al (120 nm) (electron-only), ITO/Host (80 nm)/TAPC (10 nm)/Al (120 nm) (hole-only). (B) The absorption spectrum of PO-01 and the emission spectrum of 26-TPA2P, measured in toluene.

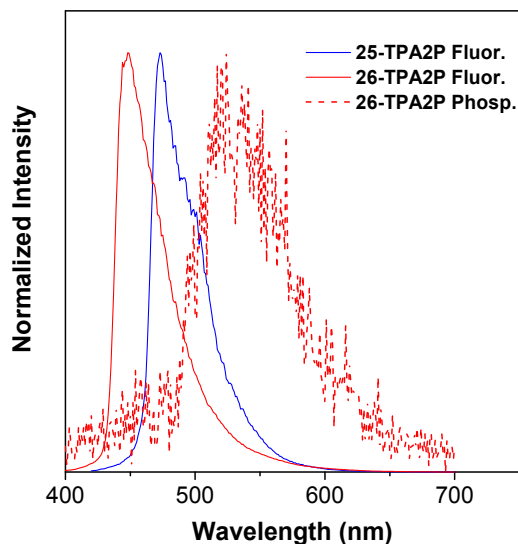


Fig. S12 The fluorescence spectra of 25-TPA2P and 26-TPA2P at 77K; the phosphorescence spectrum of 26-TPA2P at 77K (delay by 1 ms). And failed to attain the phosphorescence spectra of 25-TPA2P.

Table S4. E_{S1} and E_{T1} of 25-TPA2P and 26-TPA2P.

Compounds	E_{S1} (eV)	E_{T1} (eV)
25-TPA2P	2.69	N.D.
26-TPA2P	2.87	2.59

Table S5. EL performance of phosphorescent OLEDs based on the PO-01 and Ir(piq)₂acac.

Device	λ_{EL} (nm)	V_{on} (V) ^b	L (cd/m ²) ^a	η_C (cd/A) ^a	η_P (lm/W) ^a	η_{ext} (%) ^a	CIE (x, y) ^c
O4	558	2.7	>60000	82.00	80.51	25.05	(0.48,0.51)
R1	620	2.7	10160	11.57	12.99	13.08	(0.68,0.33)
R2	622	2.7	10240	10.10	10.49	11.77	(0.67,0.33)

^a The luminescence (L), current efficiency (η_C), power efficiency (η_P) and external quantum efficiency (η_{ext}) are the maximum values of the devices. ^b V_{on} is the turn-on voltage at 1 cd/m². ^c CIE coordinates at current density of 10 mA/cm². ^d Since the maximum luminescence range of the test instrument (PR745) is only 60,000 cd/m². Device configuration: ITO/HATCN (5 nm)/TAPC (50 nm)/TcTa (5 nm)/26-TPA2P (12 nm)/26-TPA2P: 3wt%PO-01 (8 nm)/TmPyPB (40 nm)/LiF (1nm)/Al (120 nm) (Device O4); ITO/HATCN (5 nm)/TAPC (50 nm)/TcTa (5 nm)/26-TPA2P: 3wt%Ir(piq)₂acac (8 nm)/TmPyPB (40 nm)/LiF (1nm)/Al (120 nm) (Device R1) and ITO/HATCN (5 nm)/TAPC (50 nm)/TcTa (5 nm)/26-TPA2P: 5wt%Ir(piq)₂acac (8 nm)/TmPyPB (40 nm)/LiF (1nm)/Al (120 nm) (Device R2).

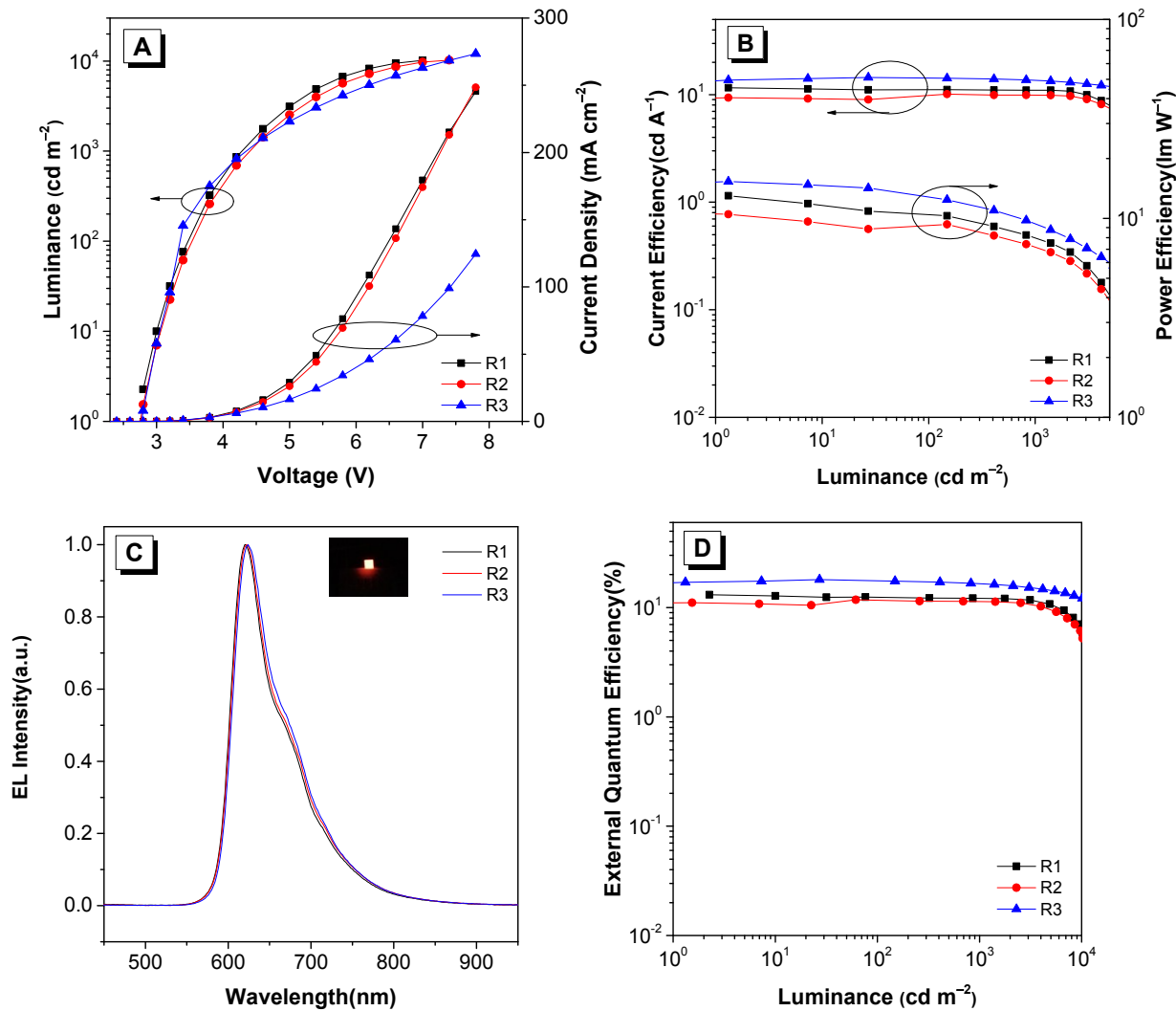


Fig. S13 (A) luminance and current density changed curves with the change of voltage of red devices. (B) current efficiency and power efficiency changed curves with the change of luminance of red devices. (C) Normalized EL spectra curves of electroluminescent devices, measured at 10 mA/cm². (D) external quantum efficiency changed curves with the change of luminance of red devices.

Table S6. Summary of performances of the fabricated two-color hybrid WOLEDs.

Device	λ_{EL} (nm)	V_{on} (V) ^b	L (cd/m ²) ^a	η_C (cd/A) ^a	η_P (lm/W) ^a	η_{ext} (%) ^a	CIE (x, y) ^c	CCT ^d	CRI ^e	η_{ext} @1000(%) ^e
W1	556	2.7	28860	59.75	67.04	17.71	(0.44, 0.49)	3703	34	13.95
W2	556	2.7	35310	26.28	22.65	9.45	(0.41, 0.42)	3826	41	8.99
W3	556	2.7	15590	17.14	12.89	6.45	(0.34, 0.35)	5085	58	5.64
W4	556	2.5	>60000	80.81	94.81	23.70	(0.45, 0.50)	3459	33	15.72
W5	556	2.5	47690	84.41	94.82	24.84	(0.44, 0.49)	3795	33	17.02
W6	556	2.5	32850	85.27	95.68	25.12	(0.40, 0.43)	4484	34	15.65
W7	556	2.7	20560	93.26	104.64	27.69	(0.38, 0.41)	6171	37	12.30

^a The luminescence (L), current efficiency (η_C), power efficiency (η_P) and external quantum efficiency (η_{ext}) are the maximum values of the devices. ^b V_{on} is the turn-on voltage at 1 cd/m². ^c CIE coordinates at current density of 10 mA/cm². ^d CCT acquire

at 10000 cd/m². e CRI and η_{ext} @1000 cd/m². Device configuration: ITO/HATCN (5 nm)/TAPC (50 nm)/TcTa (5 nm)/26-TPA2P: 3wt%PO-01(L₁ nm)/TcTa (3 nm)/26-TPA2P (L₂ nm)/TmPyPB (40 nm)/LiF (1nm)/Al (120 nm) (Device W1: L₁=12, L₂=8; W2: L₁=10, L₂=10; W3: L₁=8, L₂=12); ITO/HATCN (5 nm)/TAPC (50 nm)/TcTa (5 nm)/26-TPA2P: 3wt%PO-01 (L₃ nm)/TcTa (3 nm)/CBP:5wt%26-TPA2P (L₄ nm)/TmPyPB (40 nm)/LiF (1nm)/Al (120 nm) (Device W4: L₃=12 nm, L₄=8 nm; W5: L₃=10 nm, L₄=10 nm; W6: L₃=8 nm, L₄=12 nm; W7: L₃=6 nm, L₄=14 nm)

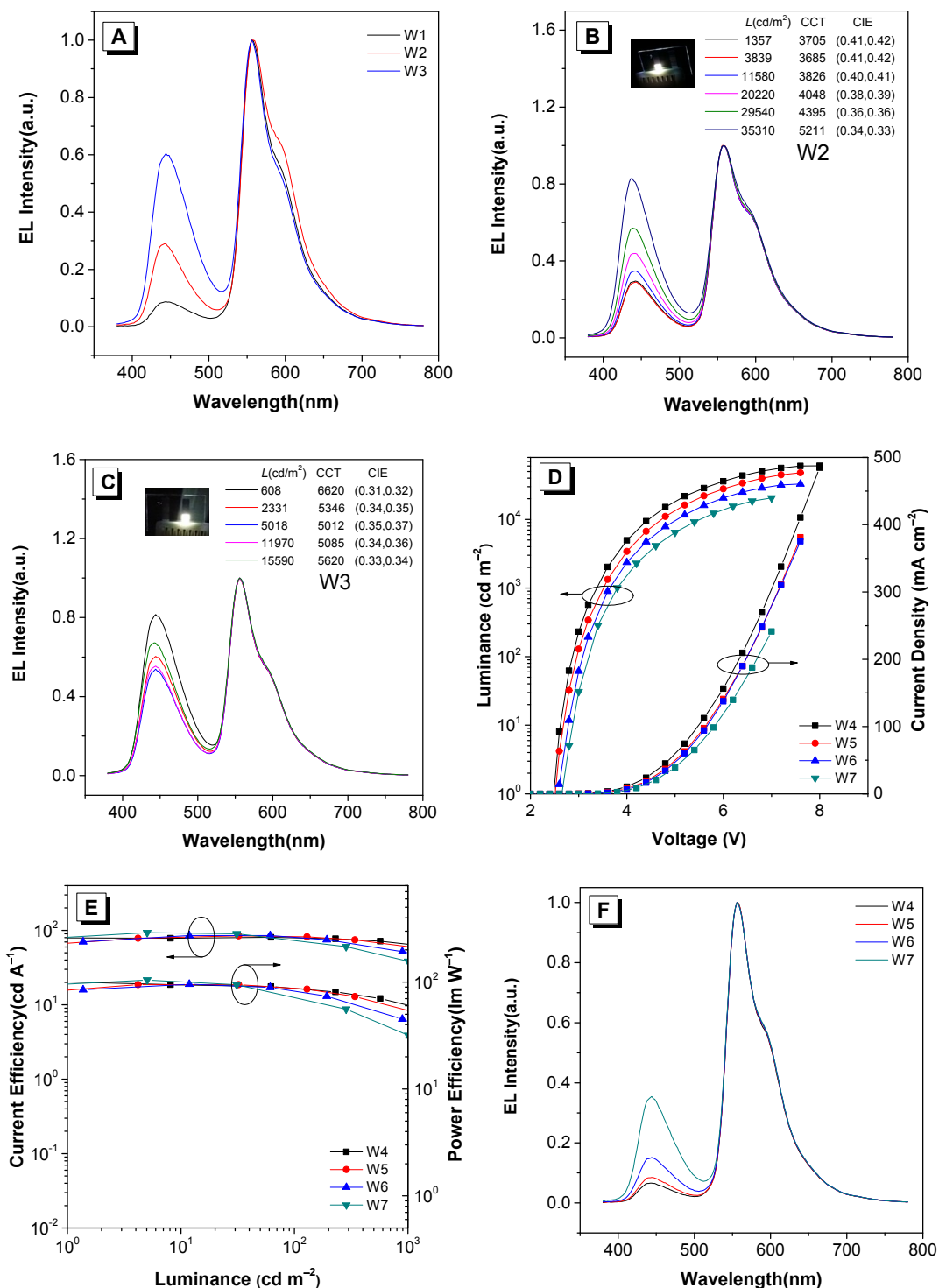


Fig. S14 (A) Normalized EL spectra of W1~W3, measured at 10 mA/cm². (B) Normalized EL spectra of device W2 at different luminance. (C) Normalized EL spectra of device W3 at different luminance. (D) Luminance and current density changed curves with the change of voltage of devices. (E) Current efficiency and power efficiency changed curves with the change of luminance of devices. (F) Normalized EL spectra curves of electroluminescent

devices(W4~W7), measured at 10 mA/cm².

Table S7. Summary of recent performances of two-color WOLEDs with high efficiency

Device	V_{on} (V) ^a	η_P (lm/W) ^b	η_{ext} (%) ^b	CIE (x, y) ^c
This work	2.7	67.04	17.71	(0.44, 0.49)
This work	2.7	104.64	27.69	(0.38,0.41)
Ref 1	2.4	73.00	19.50	(0.41, 0.48)
Ref 2	2.3	79.00	22.80	(0.44,0.47)
Ref 3	2.6	59.60	20.50	(0.33,0.41)
Ref 4	2.6	94.80	27.50	(0.45,0.46)
Ref 5	2.7	95.00	28.50	(0.45,0.48)
Ref 6	2.5	47.90	16.50	(0.46,0.47)
Ref 7	2.6	99.90	25.60	(0.43,0.44)
Ref 8	2.5	69.70	21.40	(0.44,0.45)
Ref 9	2.4	97.10	22.50	(0.40,0.49)
Ref 10	2.4	95.30	22.80	(0.36,0.50)
Ref 11	3.2	28.20	12.29	(0.42,0.46)
Ref 12	2.7	48.30	25.60	(0.41,0.46)

^a V_{on} is the turn-on voltage at 1 cd/m². ^b The power efficiency (η_P) and external quantum efficiency(η_{ext}) are the maximum values of the devices. ^c CIE coordinates at current density of 1000 cd/m² or 10 mA/cm².

6. References

1. Y. Zhang, Q. Ran, Q. Wang, J. Fan, L. Liao, *J. Mater. Chem. C*, 2019, **7**, 7267.
2. S. Ying, P. Pang, S. Zhang, Q. Sun, Y. Dai, X. Qiao, D. Yang, J. Chen, D. Ma, *ACS Appl. Mater. Interfaces*, 2019, **11**, 31078.
3. Z. Wu, Y. Liu, L. Yu, C. Zhao, D. Yang, X. Qiao, J. Chen, C. Yang, H. Kleemann, K. Leo, D. Ma, *Nat. Commun.*, 2019, **10**, 2380.
4. C. Cao, W. Chen, J. Chen, L. Yang, X. Wang, H. Yang, B. Huang, Z. Zhu, Q. Tong, C. Lee, *ACS Appl. Mater. Interfaces*, 2019, **11**, 11691.
5. Q. Tian, L. Zhang, Y. Hu, S. Yuan, Q. Wang, L. Liao, *ACS Appl. Mater. Interfaces*, 2018, **10**, 39116.
6. B. Chen, B. Liu, J. Zeng, H. Nie, Y. Xiong, J. Zou, H. Ning, Z. Wang, Z. Zhao, B. Z. Tang, *Adv. Funct. Mater.*, 2018, **28**, 1803369
7. Z. Xu, J. Gu, X. Qiao, A. Qin, B. Z. Tang, D. Ma, *ACS Photonics*, 2018, **6**, 768.
8. J. Liang, C. Li, X. Zhuang, K. Ye, Y. Liu, Y. Wang, *Adv. Funct. Mater.*, 2018, **28**, 1707002.
9. S. Ying, J. Yao, Y. Chen, D. Ma, *J. Mater. Chem. C*, 2018, **6**, 7070.
10. S. Ying, D. Yang, X. Qiao, Y. Dai, Q. Sun, J. Chen, T. Ahamad, S. M. Alshehri, D. Ma, *J. Mater. Chem. C*, 2018, **6**, 10793.
11. Z. Wang, X.-L. Li, Z. Ma, X. Cai, C. Cai, S.-J. Su, *Adv. Funct. Mater.*, 2018, **28**, 1706922.
12. J. Liang, C. Li, X. Zhuang, K. Ye, Y. Liu, Y. Wang, *Adv. Funct. Mater.*, 2018, **28**, 1707002.